

Adrian Jonas, Thomas Meurer, Birgit Kanngießer, Ioanna Mantouvalou

Note: Reflection zone plates as highly resolving broadband optics for soft X-ray laboratory spectrometers

Open Access via institutional repository of Technische Universität Berlin

Document type

Journal article | Published version

(i. e. publisher-created published version, that has been (peer-) reviewed and copyedited; also known as: Version of Record (VOR), Final Published Version)

This version is available at

<https://doi.org/10.14279/depositonce-15601>

Citation details

This article may be downloaded for personal use only. Any other use requires prior permission of the author and AIP Publishing. This article appeared in

Jonas, A., Meurer, T., Kanngießer, B., Mantouvalou, I. (2018). Note: Reflection zone plates as highly resolving broadband optics for soft X-ray laboratory spectrometers. In Review of Scientific Instruments (Vol. 89, Issue 2, p. 026108). AIP Publishing.

and may be found at <https://doi.org/10.1063/1.5018910>.

Terms of use

This work is protected by copyright and/or related rights. You are free to use this work in any way permitted by the copyright and related rights legislation that applies to your usage. For other uses, you must obtain permission from the rights-holder(s).

Note: Reflection zone plates as highly resolving broadband optics for soft X-ray laboratory spectrometers

Cite as: Rev. Sci. Instrum. **89**, 026108 (2018); <https://doi.org/10.1063/1.5018910>

Submitted: 11 December 2017 • Accepted: 08 February 2018 • Published Online: 26 February 2018

A. Jonas, T. Meurer, B. Kanngießner, et al.



View Online



Export Citation



CrossMark

ARTICLES YOU MAY BE INTERESTED IN

[Single shot near edge x-ray absorption fine structure spectroscopy in the laboratory](#)



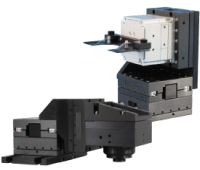
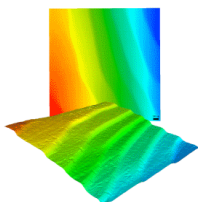
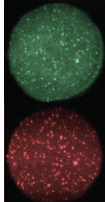
Applied Physics Letters **108**, 201106 (2016); <https://doi.org/10.1063/1.4951000>

[Off-axis reflection zone plate for quantitative soft x-ray source characterization](#)

Applied Physics Letters **71**, 190 (1997); <https://doi.org/10.1063/1.119497>

[High average power, highly brilliant laser-produced plasma source for soft X-ray spectroscopy](#)

Review of Scientific Instruments **86**, 035116 (2015); <https://doi.org/10.1063/1.4916193>

 MCL MAD CITY LABS INC. www.madcitylabs.com	<p>Nanopositioning Systems</p> 	<p>Modular Motion Control</p> 	<p>AFM and NSOM Instruments</p> 	<p>Single Molecule Microscopes</p> 
---	--	--	---	--

Note: Reflection zone plates as highly resolving broadband optics for soft X-ray laboratory spectrometers

A. Jonas, T. Meurer, B. Kanngießer, and I. Mantouvalou
TU Berlin, Analytical X-Ray Physics, D-10587 Berlin, Germany

(Received 11 December 2017; accepted 8 February 2018; published online 26 February 2018)

The resolving power and relative efficiency of two off-axis reflection zone plates (RZPs) in the soft X-ray range between 1 nm and 5 nm were investigated. RZPs focus only a very narrow bandwidth around the design wavelength. By misaligning the RZP, the focused wavelength can be tuned through a much wider spectral range. Using a laser-produced plasma source, we demonstrate that a single RZP can be efficiently used for spectroscopy at arbitrary wavelengths in the investigated soft X-ray range. *Published by AIP Publishing.* <https://doi.org/10.1063/1.5018910>

Soft X-ray spectroscopy in the range between 1 nm and 5 nm (1200 eV–200 eV) is still most commonly performed at large scale facilities. This is due to the lack of efficient laboratory sources for the soft X-ray region. To meet the increasing demand for spectroscopic techniques such as near edge X-ray absorption fine structure (NEXAFS) spectroscopy, efforts are conducted to design efficient experimental setups in the laboratory.

One possibility is to use highly brilliant laser-produced plasma (lpp) sources which deliver isotropic broadband radiation.^{1,2} For the diagnostics of such sources but also for the envisioned spectroscopic techniques, adapted spectrometers are needed with both high resolving power (RP) and broadband efficiency. In most published work, the dispersive element used for spectroscopy is either a transmission grating^{3,4} or a concave [variable line-spaced (VLS)] grating.^{5,6} In recent years, reflection zone plates (RZPs) have been shown to enable efficient soft X-ray spectroscopy with laboratory sources such as single shot NEXAFS⁷ due to their high reflectivity and large numerical aperture. These two-dimensional grating structures can be used for focusing,⁸ imaging,⁹ and dispersing¹⁰ of X-radiation. Up until now, though, specially designed RZPs for specific energy regions are utilized⁷ due to a fast degeneration of RP caused by chromatic aberration, necessitating many high-priced optics if several absorption edges are of interest.

We report that by misaligning the setup geometry, the usable wavelength range can be varied between 1 nm and 5 nm without notable loss in efficiency or RP. The full wavelength range can be covered by one single RZP structure in sequential measurements. To illustrate this behavior, emission spectra of tungsten and copper obtained with a lpp source using two different RZP structures are shown with different setup geometries. The setup utilizes a laboratory lpp source described in Ref. 11, where a 1 ns, 100 Hz Yb:YAG thin disk laser (1030 nm) is used to produce soft X-rays in the range of 1 nm–5 nm with a variable emission spectrum.¹² The high vacuum spectrometer consists of the RZP structures, a CCD camera (GE 2048 512 X-ray, Greates GmbH), and a 200 nm Al filter which eliminates visible and IR light. The two RZP structures which were designed for the investigation of the C and N K edge at 4.4 nm and 3 nm, respectively, with an

object distance F_1 of 1500 mm and an image distance F_2 of 2500 mm are written on the same substrate and are thus exchangeable by a translation of the optic. They can be additionally rotated in two directions and the CCD camera can be aligned in 3D.

The RZP structure focusses only on radiations with the design wavelength in the CCD plane. The image of other wavelengths is broadened in the vertical as well as the horizontal direction, resulting in a cross shaped pattern on the CCD; see Fig. 1. This allows long image distances F_2 without losing detectable solid angle. Because only the outer part (off-axis) of the actual RZP structure is used, the grating period d varies only slightly. Therefore, the conventional grating formula can be used in good approximation. The grating period in the middle of the RZP structure is 3.054 μm for C and 2.115 μm for N resulting in a linear dispersion $dx/d\lambda$ of 13 mm/nm and 19 mm/nm, respectively. With a 25.4 mm long CCD chip, a wavelength range of approximately 1.5 nm can be detected. For the measurement of the full lpp spectrum between 1 nm and 5 nm, the CCD must be shifted several centimeters along the dispersion axis. Using the grating formula and geometric considerations, the RP can be expressed by

$$\frac{\lambda}{\Delta\lambda} = \frac{F_2 \lambda}{S d \sin(\beta)}.$$

Here, S stands for the effective source size and β is the diffraction angle. With $F_2 = 2500$ mm and $S = 50$ μm (FWHM), $\lambda/\Delta\lambda$ of about 1100 at the design wavelength λ for both RZP structures is expected. The RP peaks at the design wavelength and degenerates linearly in x and y to both sides, which is equivalent to $1/\lambda$ for small $d\lambda$. By changing either F_2 or β , the focused wavelength in the detector plane can be changed. This ultimately tunes the wavelength of maximum RP, so other wavelengths can be measured by misaligning the experimental setup. Changing F_2 is not advisable because the misalignment for a notable change of focused wavelength is in the order of a couple of meters. The diffraction angle β , on the other hand, only has to be changed a few mrad for a focus wavelength change of 0.1 nm. By introducing an aperture, the depth of the field can be increased, resulting in a slower degeneration of the RP. This can be accomplished with a knife edge which is placed in the middle of the RZP structure

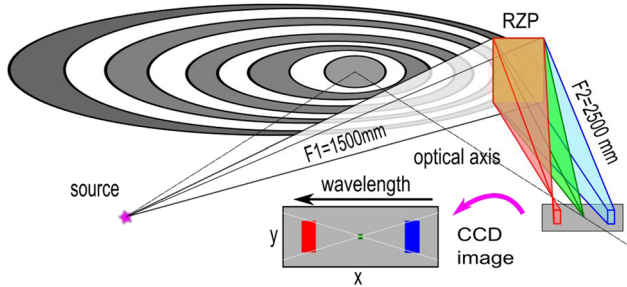


FIG. 1. Schematic view of the spectrometer principle. Different wavelengths are focused at different positions on the optical axis.

perpendicular to the grooves. Assuming a 0.25 mm distance between the knife edge and the RZP structure, the aperture is reduced by a factor of 10 with an accompanying tenfold reduction of intensity. Due to the intrinsic RZP structure, the number of illuminated grooves is not reduced, therefore preserving the RP. The calculated average efficiency for the used optics is 17.4% for the C structure and 17.1% for the N structure. It is dependent of the line density, angle of incidence, the silicon wafer surface properties, and the grating profile depth.⁵

To acquire the spectrum from the CCD image, the background is subtracted and the counts in each pixel row are summed up. This simple summarization is well justified due to the negligible curvature of the equi-energy lines near the horizontal focus. For the determination of the relative efficiency, the whole plasma emission range from 1 nm to 5 nm was measured by moving the detector along the direction of dispersion. The angle of the RZP was optimized to focus 2.5 nm vertically in the middle of the CCD. Because of the limited size of the CCD chip size, the CCD had to be shifted three times. The aperture was decreased by a factor of ten to increase the RP out of focus. Despite the closed aperture, the measuring time with 120 mJ of laser energy was between 0.5 s and 10 s, depending on the distance to the horizontal focus. The wavelength axis was calibrated using the NIST database for the atomic copper lines. Measurements were performed with both RZP structures (C, N) successively and copper as well as tungsten as the target material; see Fig. 2. As the setup is not fully calibrated, only the relative efficiency can be discussed. For comparison, a spectrum that has been collected with a VLS spectrometer (description see Ref. 7) is shown.

The y-axis is normalized to the acquisition time and the NA of the RZP structure. No correction was performed concerning the filter and the CCD as they were used for all measurements. The shape of the spectra is similar for the reference spectrum and the spectrum collected with the C structure. The efficiency of the N structure decreases to smaller wavelengths, which is contrary to a possible efficiency decrease with distance to the design wavelength. This behavior is presumed to originate from diffraction effects caused by the profile depth or the quality of the structure.

To determine the RP, isolated lines in the Cu spectrum can be used by calculating the FWHM of the respective lines. The hereby obtained values are the lower limit for the RP because the natural linewidth is neglected. The achieved RP

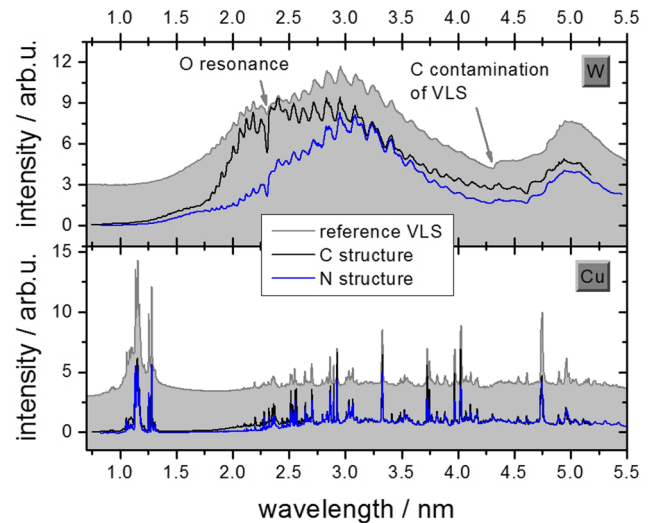


FIG. 2. Tungsten (top) and copper (bottom) plasma emission spectrum obtained with the N (blue) and C (black) RZP structures and a VLS spectrometer (grey). The VLS grating has a C containing contamination layer visible in a C K-edge feature in the spectrum. The RZP structures show O contamination.

while peaking at the design wavelength and degrading to both higher and lower wavelengths is for all wavelengths better than $\lambda/\Delta\lambda = 140$, comparable to the lower performance of commercially available VLS gratings.

For the determination of the optimally achievable RP, several measurements with different RZP angles and open aperture were conducted. Figure 3 presents an example on how the spectrum changes with different RZP angles and emphasizes the small depth of the field with open aperture. The copper spectrum measured with the N-RZP is shown. The spectrum consists of Cu relaxation lines from up to 20-times ionized Cu. The focus wavelength clearly moves between the two measurements. The change is most notably for the Cu XX line doublet at 1.257 nm and 1.2827 nm belonging to 2p-3s transitions.

The determination of the RP for selected isolated atomic lines over the whole spectral range is shown with the help of ten single overlapping measurements (depicted with different line

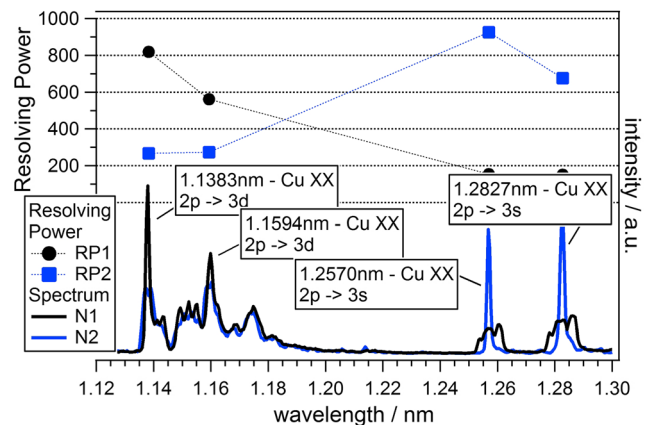


FIG. 3. Copper spectrum around 1.2 nm measured with the N-RZP at two different RZP angles. The full aperture was used and the RP for four selected lines is depicted.

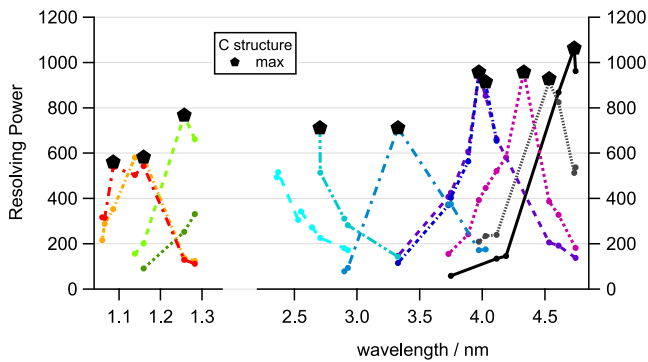


FIG. 4. RP for selected isolated plasma lines at different setup geometries measured with the C structure.

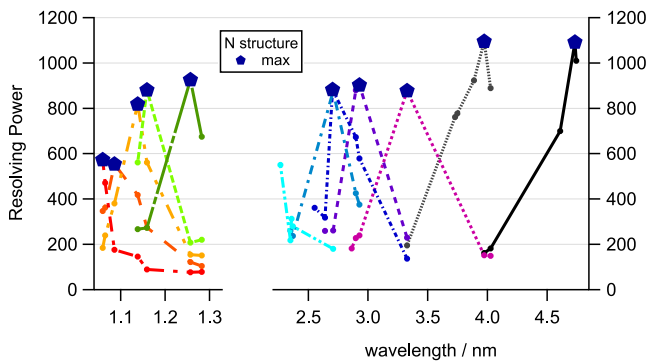


FIG. 5. RP for selected isolated plasma lines at different setup geometries measured with the N structure.

style) in Fig. 4 (C structure) and Fig. 5 (N structure). For each measurement, the fast degeneration of the RP is evident. The highest determined RP for each measurement is marked with a pentagram. Please note that there are no atomic lines between 1.3 nm and 2.4 nm available in the spectrum. The maximum measured RP for both RZP structures degenerates from around 1100 at 4.7 nm to 600 at 1.05 nm. These values must be taken as the lower limit, as for some of the measurements, suitable isolated lines are missing; see Fig. 1. The N-RZP shows a higher overall performance. There seems to be no correlation between RP and RZP structure design energy.

The usability of a single RZP structure as a broadband dispersive element for soft X-ray spectroscopy was demonstrated. By misaligning the structure and collecting the spectra sequentially, the range between 1 nm and 5 nm can be covered with a high efficiency ($>10\%$) and RP (>600). Compared to widely used VLS gratings, an improvement of a factor of 2–4 was achieved. As RZP structure sizes are limited to lines/mm depending on the manufacturing technique, and this is different for different design wavelengths, the use of one RZP structure designed for center wavelength of the source emission might be advantageous for efficient spectroscopy at arbitrary wavelengths in the investigated soft X-ray range.

The authors thank H. Stiel, H. Löchel, and A. Erko for fruitful discussions. The work was conducted in the framework of DFG Project No. 313838950.

- ¹G. M. Zeng, H. Daido, K. Murai, Y. Kato, M. Nakatsuka, and S. Nakai, *J. Appl. Phys.* **72**, 3355 (1992).
- ²I. Mantouvalou, R. Jung, J. Tuemmler, H. Legall, T. Bidu, H. Stiel, W. Malzer, B. Kanngiesser, and W. Sandner, *Rev. Sci. Instrum.* **82**, 66103 (2011).
- ³D. Adjei, M. G. Ayele, P. Wachulak, A. Bartnik, Ł. Węgrzynski, H. Fiedorowicz, L. Vyšín, A. Wiechec, J. Lekki, W. M. Kwiatek, L. Pina, M. Davidková, and L. Juha, *Nucl. Instrum. Methods Phys. Res., Sect. B* **364**, 27 (2015).
- ⁴A. S. Moore, T. M. Guymer, J. L. Kline, J. Morton, M. Taccetti, N. E. Lanier, C. Bentley, J. Workman, B. Peterson, K. Mussack, J. Cowan, R. Prasad, M. Richardson, S. Burns, D. H. Kalantar, L. R. Benedetti, P. Bell, D. Bradley, W. Hsing, and M. Stevenson, *Rev. Sci. Instrum.* **83**, 10E132 (2012).
- ⁵C. Fujikawa, N. Yamaguchi, T. Hara, T. Kawachi, H. Oyama, K. Ando, and Y. Aoyagi, *Rev. Sci. Instrum.* **69**, 2849 (1998).
- ⁶M. Müller, F.-C. Köhl, P. Großmann, P. Vrba, and K. Mann, *Opt. Express* **21**, 12831 (2013).
- ⁷I. Mantouvalou, K. Witte, W. Martyanov, A. Jonas, D. Grötzsch, C. Streeck, H. Löchel, I. Rudolph, A. Erko, H. Stiel, and B. Kanngießer, *Appl. Phys. Lett.* **108**, 201106 (2016).
- ⁸M. Ibek, T. Leitner, A. Erko, A. Firsov, and P. Wernet, *Rev. Sci. Instrum.* **84**, 103102 (2013).
- ⁹C. Braig, H. Löchel, A. Firsov, M. Brzhezinskaya, A. Hafner, J. Rehanek, M. Wojcik, A. Macrander, L. Assoufid, and A. Erko, *Opt. Lett.* **41**, 29 (2016).
- ¹⁰T. Wilhein, D. Hambach, B. Niemann, M. Berglund, L. Rymell, and H. M. Hertz, *Appl. Phys. Lett.* **71**, 190 (1997).
- ¹¹I. Mantouvalou, K. Witte, D. Grötzsch, M. Neitzel, S. Günther, J. Baumann, R. Jung, H. Stiel, B. Kanngiesser, and W. Sandner, *Rev. Sci. Instrum.* **86**, 35116 (2015).
- ¹²I. Mantouvalou, A. Jonas, K. Witte, R. Jung, H. Stiel, and B. Kanngießer, *Proc. SPIE* **10243**, 1024308 (2017).